Compact Wideband Filtering Power Dividers Based on Short-Circuited Stubs

Gaoya Dong, Bo Zhang, Weimin Wang, and Yuanan Liup

Beijing Key Laboratory of Work Safety Intelligent Monitoring
Beijing University of Posts and Telecommunications, Beijing 100876, China
gaoyadong@bupt.edu.cn, zhangbo2008beiyou@bupt.edu.cn, wangwm@bupt.edu.cn, yuliu@bupt.edu.cn

Abstract ─ A novel circuit is proposed to design filtering power dividers (FPDs) with bandpass filtering responses and out-of-band rejection performances. The presented circuit is constructed of two transmission line sections, four short-circuited sections and one resistor. Based on the introduced novel circuit, FPD1 is designed by selecting transmission line sections and short-circuited sections as quarter-wave transmission lines. The FPD2 is proposed to realize more compact size, enhanced bandpass selectivity and improved out-of-band rejection performance by replacing the quarter-wave transmission lines in FPD1 with dual transmission lines. The corresponding equations are derived to calculate the initial parameter values of FPD1 and FPD2 by adopting even-odd mode method. For verification, two FPDs centered at 2.0 GHz are designed and fabricated. The measured 3-dB fractional bandwidths of FPD1 and FPD2 achieve up to 63.2% and 52.3%, while the measured rejections with the level better than 20 dB extend to $2.4f_0$ and $4.0f_0$, respectively.

Index Terms ─ Filtering response, high selectivity, out-of-band rejection, power divider.

I. INTRODUCTION

Power dividers and bandpass filters play important roles in modern microwave systems. By integrating two functions of power division and filtering response in only one component, the passband insertion loss and construction size can be reduced effectively. Recently, many efforts have been done to realize dual functions in only one component, i.e., filtering PDs [1-8]. Various stub-loaded resonators are utilized in [1-5] to design FPDs. In [6], Wilkinson PD integrated with bandpass filter is presented to design FPD. Source-loading coupling is adopted in [7] to generate transmission zeros, ensuring high bandpass selectivity. Moreover, FPD is proposed in [8] based on right-/left-handed transmission line resonators, which can not only split the microwave signals, but also provide filtering performance.

In modern communication system, out-of-band rejection performance is greatly demanded to suppress the interferences, i.e., intermodulation signals from nonlinear components. Thus, many studies [9-14] have been done to design PDs integrated with harmonic suppression performances. Open-circuited stubs are employed in [9-10] to build PDs with enhanced spurious suppressions. In addition, coupled lines and non-uniform transmission lines are introduced in [11] and [12] to obtain harmonic suppression performances. In [13-14], low-pass filter and front coupled tapered compact microstrip resonant cell (FCTCMRC) are inserted into quarter-wave transmission lines of conventional Wilkinson PDs to realize good out-of-band rejections.

From the discussion above, PDs integrated with filtering responses and out-of-band rejections are popular and desirable. Some efforts [15-19] have been made to design FPDs with out-of-band rejections, which could suppress the unwanted high-frequency signals. The structure proposed in [15] is embedded with dual-mode resonators to obtain out-of-band rejection, and the filtering response is obtained by combining the filter with the power divider together. In [16-19], stub-loaded resonators are introduced to create transmission zeros (TZs) in stopband, resulting in good out-of-band rejections. The structure presented in [17] achieves the best out-of-band rejection performance among the five structures introduced in [15-19], where the upper stopband extends to $2.7f_0$ with the level better than 23 dB. Thus, simple design method for FPDs with better out-of-band rejections is demanded.

In this work, FPD1 and FPD2 are proposed based on the designed basic FPD circuit. The upper stopband of FPD1 (FPD2) extends to $2.4f_0$ ($4.0f_0$) with the level better than 20 dB. Even-odd mode method is adopted to analyze the operating mechanisms of FPD1 and FPD2, and the corresponding equations are derived to calculate the initial parameter values of FPDs. Based on the mentioned above, two FPDs with good out-of-band rejections are designed based on simple design methods.

II. STRUCTURE AND THEORY

A. Analysis of basic FPD circuit

The schematic of the proposed basic FPD circuit is shown in Fig. 1. Even-odd mode method is adopted to explain the operating mechanisms of basic FPD circuit.

Submitted On: May 25, 2017
Accepted On: December 24, 2018

1054-4887 © ACES

Under even-mode excitation, the power input from port 1 will be totally transmitted to port 2 and port 3 with no current flowing through insolation resistor R. Thus, the even-mode equivalent circuit of basic FPD circuit is exhibited in Fig. 1 (b). The symmetrical plane can be seen as virtual ground under odd-mode excitation, and the odd-mode equivalent circuit of basic FPD circuit is described in Fig. 1 (c).

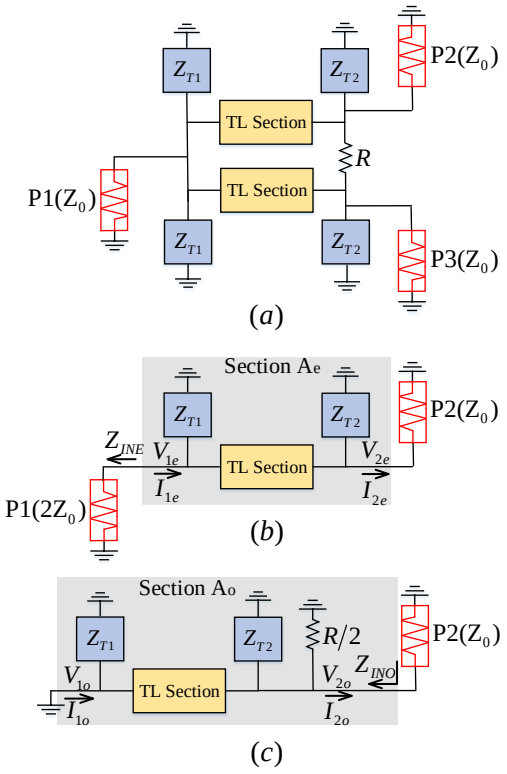

Fig. 1. Proposed basic FPD circuit: (a) the schematic of basic FPD circuit, (b) even-mode equivalent circuit of basic FPD circuit, and (c) odd-mode equivalent circuit of FPD circuit.

Define $Z_{T1} = 1/jX_{T1}$ and $Z_{T2} = 1/jX_{T2}$. From the even-mode equivalent circuit shown in Fig. 1 (b), the $A_eB_eC_eD_e$ matrix can be deduced as equation (1). Based on transmission line theory and equivalent even-mode circuit displayed in Fig. 1 (b), the input impedance in port 1 (Z_{INE}) can be derived as equation (2). Thus, S_{11} and S_{21} can be expressed as equation (3):

$$\begin{bmatrix} A_e & B_e \\ C_e & D_e \end{bmatrix} = \begin{bmatrix} 1 & 0 \\ \dfrac{1}{jX_{T1}} & 1 \end{bmatrix} \begin{bmatrix} A_{TL} & B_{TL} \\ C_{TL} & D_{TL} \end{bmatrix} \begin{bmatrix} 1 & 0 \\ \dfrac{1}{jX_{T2}} & 1 \end{bmatrix}, \quad (1)$$

$$Z_{INE} = \frac{X_{T1}(X_{T2}F - jB_{TL}Z_0)}{X_{T1}X_{T2}E - jX_{T2}F - (jX_{T1}D_{TL} + B_{TL})Z_0}, \quad (2)$$

where

$$E = C_{TL}Z_L + D_{TL},$$

$$F = A_{TL}Z_L + B_{TL},$$

$$S_{11} = \left| \frac{Z_{INE} - 2Z_0}{Z_{INE} + 2Z_0} \right|, \quad (3a)$$

$$S_{21} = \sqrt{1 - \left(\frac{Z_{INE} - 2Z_0}{Z_{INE} + 2Z_0} \right)^2}. \quad (3b)$$

The expression $A_oB_oC_oD_o$ matrix can be derived as equation (4) based on odd-mode equivalent circuit depicted in Fig. 1 (c). According to equations (4) and transmission line theory, the input impedance in port 2 (Z_{INO}) can be calculated as equation (5). Thus, S_{22} can be expressed as equation (6):

$$\begin{bmatrix} A_o & B_o \\ C_o & D_o \end{bmatrix} = \begin{bmatrix} A_{TL} & B_{TL} \\ C_{TL} & D_{TL} \end{bmatrix} \begin{bmatrix} 1 & 0 \\ \dfrac{1}{jX_{T2}} & 1 \end{bmatrix} \begin{bmatrix} 1 & 0 \\ \dfrac{2}{R} & 1 \end{bmatrix}, \quad (4)$$

$$Z_{INO} = \frac{B_{TL}X_{T2}R}{X_{T2}(A_{TL}R + 2B_{TL}) - jB_{TL}R}, \quad (5)$$

$$S_{22} = \left| \frac{Z_{INO} - Z_0}{Z_{INO} + Z_0} \right|. \quad (6)$$

B. Analysis of FPD1

Based on basic FPD circuit, FPD1 is presented by selecting TL section, Z_{T1} and Z_{T2} as quarter-wave transmission lines. The schematic of FPD1 is shown in Table 1, which consists of two quarter-wave transmission lines (Z_1, θ), four short-circuited transmission lines (Z_2, θ) and one isolation resistor (R_1), and all electrical lengths (θ) of transmission lines are selected as $\pi/2$ at the center frequency (f_0). According to the schematic of FPD1, $A_{TL}B_{TL}C_{TL}D_{TL}$ matrix, X_{T1} and X_{T2} can be expressed as equation (7). The expressions of Z_{INE} and Z_{INO} can be derived as equation (8) by submitting equation (7) into equations (2) and (5). In a specific case, Z_{INE} and Z_{INO} in FPD1 can be simplified as Z_1^2/Z_0 and $R_1/2$ at f_0, respectively. Thus, the initial value of Z_1 should be chosen as $\sqrt{2}Z_0$ to realize good impedance matching in port 1 under even-mode excitation, and the initial value of R_1 should be selected as $2Z_0$ to obtain good impedance matching in port 2 under odd-mode excitation. Thus, the initial values of Z_1 and R_1 are calculated as 70.7 Ω and 100 Ω when Z_0 is adopted as 50 Ω:

Table 1: Summary of proposed FPD1 and FPD2

	Schematic	Layout	Normalized Frequency Response
FPD1	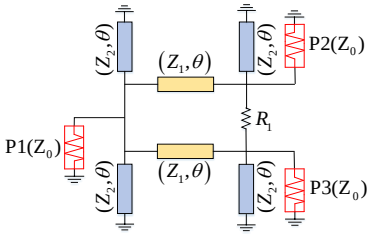	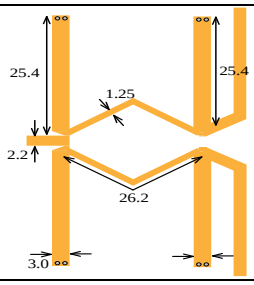	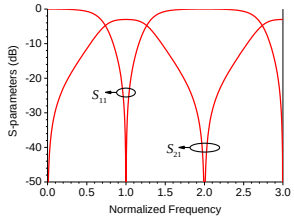
FPD2	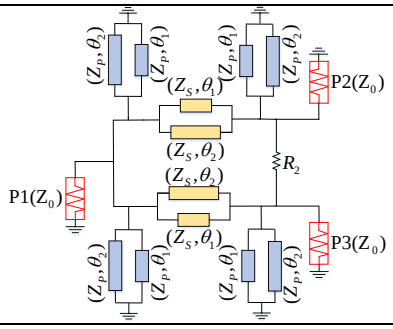	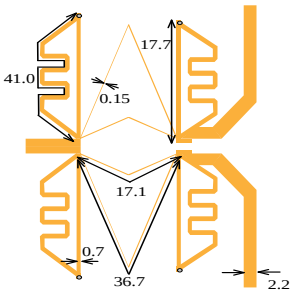	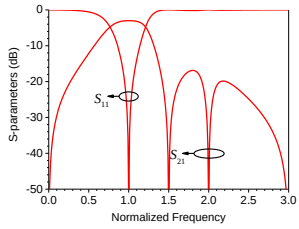

$$\begin{bmatrix} A_{TL} & B_{TL} \\ C_{TL} & D_{TL} \end{bmatrix} = \begin{bmatrix} \cos\theta & jZ_1\cos\theta \\ jY_1\sin\theta & \cos\theta \end{bmatrix}, \quad (7a)$$

$$X_{T1} = Z_2\tan\theta\,, \quad (7b)$$

$$X_{T2} = Z_2\tan\theta\,, \quad (7c)$$

$$Z_{INE} = \frac{Z_0Z_1Z_2\cos\theta(Z_1+Z_2)+j(Z_1Z_2\sin\theta)^2}{2(Z_1Z_2\sin\theta\cos\theta(Z_1+Z_2)+jZ_0((Z_2)^2-(\cos\theta)^2(Z_1+Z_2)^2))}, \quad (8a)$$

$$Z_{INO} = \frac{jRZ_1Z_2\sin\theta}{R\cos\theta(Z_1+Z_2)+2jZ_1Z_2\sin\theta}. \quad (8b)$$

Transmission zeros could be obtained when $S_{21}=0$. According to the equations (3) and (7), the frequencies of TZs in FPD1 can be summarized as equation (9):

$$f_{TZn} = \left\{ 2nf_0 \mid n\in N, f>0 \mid \tan(\frac{f\theta}{f_0}) = 0 \right\}, \quad (9a)$$

$$f_{TZn} = \left\{ 2nf_0 \mid n\in N, f>0 \right\}, \quad (9b)$$

To further explain the operating mechanisms of FPD1, the normalized frequency responses with various values of Z_1 and Z_2 are shown in Fig. 2. As observed in Fig. 2 (a), the return loss of FPD1 can be optimized by choosing proper value of Z_1, which has a good agreement with equations (8a). According to Fig. 2 (b), the 3-dB fractional bandwidth (FBW) can be adjusted by tuning the value of Z_2, which agrees with equations (8a).

C. Analysis of FPD2

In order to further improve the upper stopband rejection and miniaturization performances, FPD2 is presented by replacing the quarter-wave transmission line (Fig. 3 (a)) in FPD1 with the harmonic suppression dual transmission lines (Fig. 3 (b)), and dual transmission lines have been analysed in our previous work [20]. The schematic of FPD2 is depicted in Table 1, where six pairs of dual transmission lines ((Z_S,θ_1 ; Z_S,θ_2), (Z_P,θ_1; Z_P,θ_2)) are employed, and the electrical lengths of dual transmission lines are chosen as $\theta_1=\pi/3$ and $\theta_2=2\pi/3$. Based on the equations (1-7) exhibited in paper [21], the $A_{TL}B_{TL}C_{TL}D_{TL}$ matrix of dual transmission lines can be deduced as equation (10a), and X_{T1}, X_{T2} can be expressed as (10b), (10c) respectively:

$$\begin{bmatrix} \frac{\cos\theta_1\sin\theta_2+\cos\theta_2\sin\theta_1}{\sin\theta_1+\sin\theta_2} & \frac{jZ_S\sin\theta_1\sin\theta_2}{\sin\theta_1+\sin\theta_2} \\ j\frac{(\cos\theta_1-\cos\theta_2)^2+(\sin\theta_1+\sin\theta_2)^2}{Z_S(\sin\theta_1+\sin\theta_2)} & \frac{\cos\theta_1\sin\theta_2+\cos\theta_2\sin\theta_1}{\sin\theta_1+\sin\theta_2} \end{bmatrix}, \quad (10a)$$

$$X_{T1} = Z_P\frac{\tan\theta_1\cdot\tan\theta_2}{\tan\theta_1+\tan\theta_2}, \quad (10b)$$

$$X_{T2} = Z_P\frac{\tan\theta_1\cdot\tan\theta_2}{\tan\theta_1+\tan\theta_2}, \quad (10c)$$

$$Z_{INO} = \frac{jZ_SR\sin\theta_1\cdot\sin\theta_2}{2R(\cos\theta_1\sin\theta_2+\sin\theta_1\cos\theta_2)+2jZ_S\sin\theta_1\sin\theta_2}. \quad (11)$$

In FPD2, the detailed expressions of Z_{INE} and Z_{INO} can be obtained by substituting equation (10) into equations (2) and (5), and the specific expression of Z_{INO} is shown in equation (11). In a particular case, Z_{INE} and Z_{INO} can be simplified as $3Z_S^2/16Z_0$ and $R_2/2$ at f_0. The initial value of Z_S should be selected as $4\sqrt{2/3}\,Z_0$ to obtain good impedance matching in port 1 under even-mode excitation, and the initial value of R_2 should be chosen as $2Z_0$ to realize good impedance matching in port 2 under odd-mode excitation. Thus, the initial values of Z_S and R_2 are calculated as 163.3 Ω and 100 Ω when

Z_0 is adopted as 50 Ω.

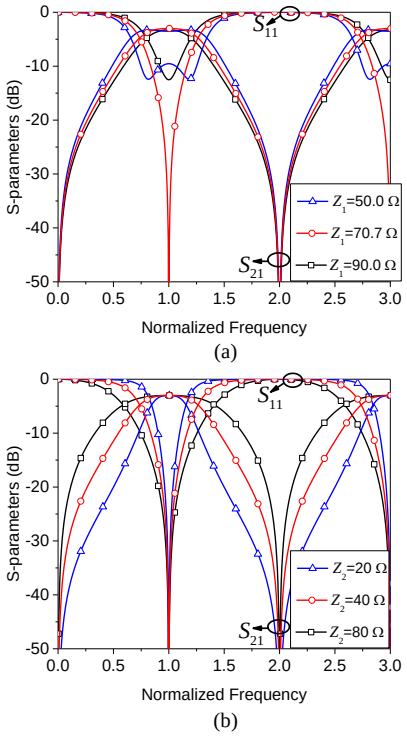

Fig. 2. Normalized frequency responses of FPD2 with various: (a) Z_1 and (b) Z_2.

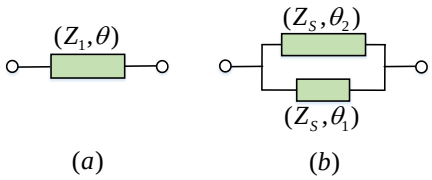

Fig. 3. Schematic of: (a) conventional quarter-wave transmission lines, and (b) dual transmission lines.

Transmission zeros could be obtained when $S_{21} = 0$. The frequencies of TZs in FPD2 can be summarized as equation (12) based on the equations (3) and (10):

$$f_{TZn}^{S} = \left\{ 2nf_0 \mid n \in N,\ f > 0 \mid \tan\left(\frac{f\theta_1}{f_0}\right) = -\tan\left(\frac{f(\pi-\theta_1)}{f_0}\right) \right\}, \quad (12a)$$

$$f_{TZn}^{P} = \left\{ \frac{n\pi f_0}{\theta_1}, \frac{n\pi f_0}{(\pi-\theta_1)}, n \in N \right\}. \quad (12b)$$

To further explain the operating mechanisms of FPD2, the normalized frequency responses with various values of Z_S and Z_P are displayed in Fig. 4. As observed in Fig. 4 (a), the return loss in FPD2 can be optimized by choosing a proper value of Z_S, which has a good agreement with equations (2-3) and (10). It can be seen from Fig. 4 (b) that 3-dB FBW can be adjusted by tuning the value of Z_P, which agrees with equations (2-3) and (10).

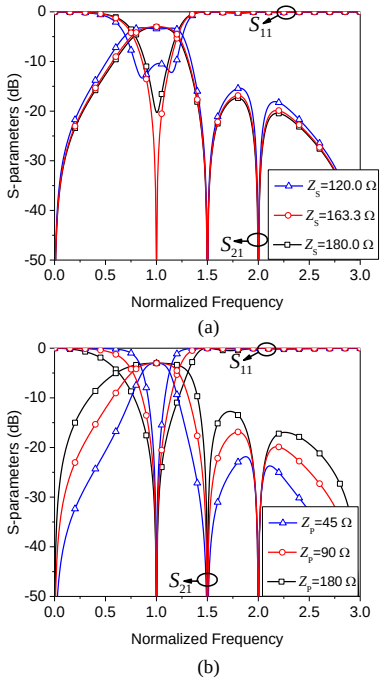

Fig. 4. Normalized frequency responses of FPD2 with various: (a) Z_S and (b) Z_P.

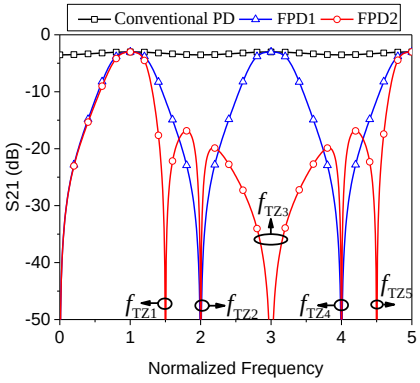

Fig. 5. Normalized frequency responses of different PD structures.

The normalized frequency responses of the conventional Wilkinson PD, FPD1 and FPD2 are plotted in Fig. 5. By comparing with conventional Wilkinson PD, good bandpass filtering response can be obtained in FPD1 and FPD2. Three additional TZs (f_{TZ1}, f_{TZ3} and f_{TZ5}) in the upper stopband are introduced in FPD2 by comparing with FPD1, which can greatly enhance the passband selectivity and improve out-of-band rejection performance. Transmission zeros depicted in Fig. 5 agree well with equations (9) and (12).

Based on the analysis above, the design procedures of the proposed FPD1 is described as following:

1) Given specific center frequency (f_0), FBW and out-of-band rejection performances of FPD1.
2) Calculate the initial values of Z_1 and R_1 based on equation (8).
3) Adjust the value of Z_2 to obtain required FBW.
4) Tune the value of R_1 to realize a good isolation between port 2 and port 3.
5) Optimize return loss in port 1 by changing the value of Z_1.
6) Return to step (3) until designed FPD1 meets the requirement required in step (1).

The detailed design procedures of FPD2 is summarized as following:

1) Given specific center frequency (f_0), FBW and out-of-band rejection performances of FPD2.
2) The initial values Z_S and R_2 are adopted as $4\sqrt{2/3}\,Z_0$ and $2Z_0$, respectively
3) Adjust the value of Z_P to realize required FBW.
4) The good isolation between port 2 and port 3 can be obtained by tuning the value of R_2.
5) Optimize return loss in port 1 by tuning the value of Z_S.
6) Return to step (3) until designed FPD2 satisfies the requirement given in step (1).

III. SIMULATION AND MEASUREMENT RESULTS

Based on design procedures listed above, FPD1 and FPD2 are fabricated at a center frequency (f_0) of 2.0 GHz. The substrate used herein has a dielectric constant of 2.55 and a thickness of 31 mil. The layouts and specific dimensions of FPD1 and FPD2 are exhibited in Table 1. Figure 6 shows the photographs of fabricated FPD1 and FPD2, where size miniaturization can be observed in FPD2 compared with FPD1.

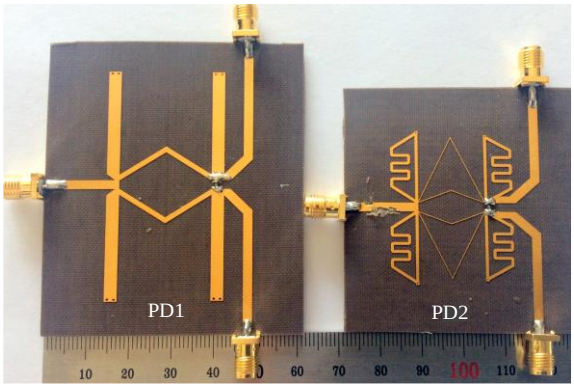

Fig. 6. Photographs of proposed FPD1 and FPD2.

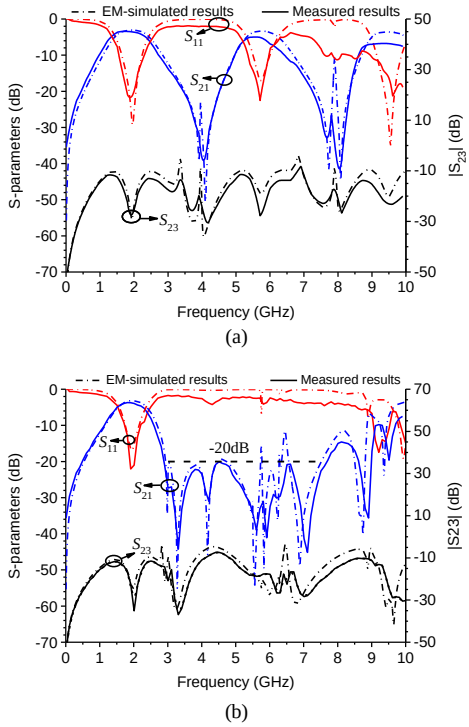

Fig. 7. EM-simulated and measured results: (a) FPD1 and (b) FPD2.

Table 2: Performance comparisons between proposed FPDs and the published works

References	FBW	Insertion Loss (dB)	Out-of-band Rejection Performance (dB)
[15]	7.2%	4.2	>20 dB (2.9 f_0)
[16]	70%	3.3	>13 dB (2.7 f_0)
[17]	8.3%	3.9	>20 dB (2.7 f_0)
[18]	5.8%	4.6	>20 dB (1.5 f_0)
[19]	6.5%	3.99	>35 dB (2.5 f_0)
FPD1	**63.2%**	**3.4**	**>20 dB (2.4 f_0)**
FPD2	**52.3%**	**3.7**	**>20 dB (4.0 f_0)**

The EM-simulated and measured results of FPD1 and FPD2 are demonstrated in Fig. 7. As shown in Fig. 7 (a), the measured FPD1 operates at the center frequency of 1.9 GHz with the 3-dB FBW of 63.2%. The measured passband return loss is better than 22 dB and the minimum insertion loss is 3.4 dB, including 3 dB power splitting loss. The measured isolation in FPD1 is better than 12 dB ranging from DC to 10 GHz which can be observed in Fig. 7 (a). The upper stopband extends up

to 4.8 GHz ($2.4f_0$) with the rejection level of better than 20 dB. As demonstrated in Fig. 7 (b), the measured minimum insertion loss in FPD2 is 3.7 dB, including 3 dB power splitting loss. The measured passband in FPD2 is centered at 1.97 GHz with the 3-dB FBW of 52.3%, while the return loss is better than 20 dB. The upper stopband in FPD2 extends up to 8 GHz ($4.0f_0$) with the rejection level of better than 20 dB. The isolation in FPD2 is better than 12 dB ranging from DC to 10 GHz.

For comparison, Table 2 lists some major performances of the published and proposed FPDs. It can be seen from Table 2 that the presented FPDs demonstrate low insertion losses, deep out-of-band rejections and wide upper stopband suppression bandwidths.

IV. CONCLUSIONS

In this paper, a novel basic FPD circuit is introduced to design FPDs. To achieve more compact size, enhanced passband selectivity and improved out-of-band rejection performance, FPD2 is presented by replacing the quarter-wave transmission lines in FPD1 with harmonic suppression dual transmission lines. The designed FPDs have the advantages of good filtering responses, wide upper stopband rejections and simple design procedures, which are suitable for practical FPD design.

ACKNOWLEDGMENT

This work was supported in part by National Natural Science Foundations of China (No. 61701041 and No. 61327806).

REFERENCES

[1] S. K. Chao and W.-C. Lin, "Filtering power divider with good isolation performance," *Electronics Letters*, vol. 50, no. 11, pp. 815-817, June 2014.

[2] H. Zhu, A. Abbosh, and L. Guo, "Wideband four-way filtering power divider with sharp selectivity and wide stopband using looped coupled-line structures," *IEEE Microwave and Wireless Components Letters*, vol. 26, no. 6, pp. 413-415, June 2016.

[3] K. Song, Y. Mo, and Y. Fan, "Wideband four-way filtering-response power divider with improved output isolation based on coupled lines," *IEEE Microwave and Wireless Components Letters*, vol. 24, no. 10, pp. 674-676, July 2014.

[4] S. W. Wong and L. Zhu, "Ultra-wideband power dividers with good isolation and sharp roll-off skirt," *Microwave Conference, 2008. APMC 2008, Asia-Pacific. IEEE*, pp. 1-4, May 2008.

[5] X. Wang, J. Wang, and G. Zhang, "Design of wideband filtering power divider with high selectivity and good isolation," *Electronics Letters*, vol. 52, no. 16, pp. 1389-1391, July 2016.

[6] L. Gao and X.-Y. Zhang, "Novel 2:1 Wilkinson power divider integrated with bandpass filter," *Microwave and Optical Technology Letters*, vol. 55, pp. 646-648, Jan. 2013.

[7] X.-L. Zhao, L. Gao, J.-X. Xu, and J. Xiang, "High-selectivity dual band filtering power divider using stub-loaded quarter-wavelength resonator," *Journal of Electromagnetic Waves and Application*, vol. 29, no. 16, pp. 2216-2223, Oct. 2015.

[8] X. Ren, K.-J. Song, B.-K. Hu and Q.-K. Chen, "Compact filtering power divider with good frequency selectivity and wide stopband based on composite right-left-handed transmission lines," *Microwave and Optical Technology Letters*, vol. 56, pp. 2122-2125, June 2014.

[9] M. Hayati and S. Roshani, "A novel Wilkinson power divider using open stubs for the suppression of harmonics," *Applied Computational Electromagnetics Society (ACES) Journal*, vol. 28, no. 6, pp.501-506, June 2013.

[10] J. Li, Y. Liu, S. Li, et al., "A novel multi-way power divider design with enhanced spurious suppression," *Applied Computational Electromagnetics Society (ACES) Journal*, vol. 29, no. 9, pp. 692-700, Sep. 2014.

[11] X. Xu and X. Tang, "Design of an ultra-wideband power divider with harmonics suppression," *International Journal of RF and Microwave Computer-Aided Engineering*, vol. 25, no. 4, pp. 299-304, Oct. 2015.

[12] K.-A. Shamaileh, A. Qaroot, N. Dib, et al., "Design of miniaturized unequal spilt Wilkinson power divider with harmonics suppression using non-uniform transmission lines," *Applied Computational Electromagnetics Society (ACES) Journal*, vol. 26, no.6, pp. 530-538, June 2011.

[13] M. Hayati, S. Roshani, S. Roshani, et al., "A novel miniaturized Wilkinson power divider with n-th harmonic suppression," *Journal of Electromagnetic Waves and Applications*, vol. 27, no. 6, pp. 726-735, Dec. 2013.

[14] M. Hayati, S. Roshani, and S. Roshani, "Miniaturized Wilkinson power divider with nth harmonic suppression using front coupled tapered CMRC," *Applied Computational Electromagnetic Society (ACES) Journal*, vol. 28, no.3, pp. 221-227, Mar. 2013.

[15] K. J. Song, "Compact filtering power divider with high frequency selectivity and wide stopband using embedded dual-mode resonator," *Electronics Letters*, vol. 56, no. 6, pp. 495-497, May 2015.

[16] B. Zhang and Y. Liu, "Wideband filtering power divider with high selectivity," *Electronics Letters*, vol. 51, pp. 1950-1952, Nov. 2015.

[17] B. Zhang, C.-P. Yu, and Y. Liu, "Compact power divider with bandpass response and improved out-of-band rejection," *Journal of Electromagnetic Waves and Application*, vol. 30, no. 9, pp. 1124-

1132, May. 2016.
[18] K. J. Song, S. Y. Hu, and C. L. Zhong, "Novel bandpass response power divider with high frequency selectivity using centrally stub-loaded resonators," *Microwave and Optical Technology Letters*, vol. 55, no.7, pp. 1560-1562, Apr. 2013.
[19] X.-Y. Zhang, K.-X. Wang, and B.-J. Hu, "Compact filtering power divider with enhanced second-harmonic suppression," *IEEE Microwave Wireless and Wireless Components Letters*, vol. 23, no. 9, pp. 483-485, Aug. 2013.
[20] B. Zhang, Y. Wu, C. Yu, and Y. Liu, "Miniaturized wideband bandpass filter based on harmonic suppressed dual transmission lines," *Electronics Letters*, vol. 52, pp. 734-736, Apr. 2016.
[21] C. W. Tang, M. G. Chen, and C. H. Tsai, "Miniaturization of microstrip branch-line coupler with dual transmission lines," *IEEE Microwave and Wireless Components Letters*, vol. 18, no. 3, pp. 185-187, Mar. 2008.

Gaoya Dong was born in Shanxi, China, in 1993. She received the B.S. degree in Applied Physics from Xidian University, Xi 'an, China, in 2015. She is currently pursuing the Ph.D. degree of Electrical Engineering in Beijing University of Posts and Telecommunications, Beijing, China.

Her current research interests include planar microwave power dividers, and antennas.

Bo Zhang was born in Shanxi, China, in 1991. He received the B.S. and M.S. degrees in Electronic and Information Engineering from the Beijing University of Posts and Telecommunications, Beijing, China, in 2012 and 2015, respectively, where he is currently working towards Ph.D. degree in Electrical Engineering.

His current research interests include planar microwave filters, power dividers, and antennas and power amplifiers.

Weimin Wang was born in Shandong, China, in 1977. She received the B.Eng. degree in Telecommunication Engineering, M.Sc. degree in Electromagnetics and Microwave Technology and the Ph.D. degree in Electronic and Information Engineering from the Beijing University of Posts and Telecommunications, Beijing, China, in 1999, 2004 and 2014, respectively.

In 2014, She joined the BUPT. She is currently a Lecturer with the School of Electronic Engineering, BUPT. Her research interests include microwave components and MIMO OTA.

Yuan Liu received the B.E., M.Eng., and Ph.D. degrees in Electrical Engineering from the University of Electronic Science and Technology of China, Chengdu, China, in 1984, 1989, and 1992, respectively.

In 1984, he joined the 26th institute of the Electronic Ministry of China to develop the inertia navigating system. In 1992, he held his first post-doctoral position with the EMC Laboratory at the Beijing University of Posts and Telecommunications (BUPT), Beijing, China. In 1995, he held his second post-doctoral position with the Broadband Mobile Laboratory at the Department of System and Computer Engineering, Carleton University, Ottawa, ON, Canada. Since 1997, he has been a Professor with the Wireless Communication Center at the College of Telecommunication Engineering, BUPT, where he is involved in the development of next-generation cellular systems, wireless LAN, Bluetooth application for data transmission, electromagnetic compatibility design strategies for high-speed digital systems, and electromagnetic interference and expected value of mean square measuring sites with low cost and high performance.